high resolution and sensitivity of this method allowed us to detect a very small percentage of Cu^{2+} polyhedra with a mixed nitro–nitrito coordination as well as the usual hexanitro species. Also the superhyperfine structure due to the interaction with the Tl nuclei was resolved in the spectra of the Tl complexes, due to a very weak spin delocalization toward the Tl^+ cations. Signals originating from exchange-coupled Cu^{2+}–Cu^{2+} pairs were observed only at higher frequencies. Finally MO parameters for the Cu–N bonds could be derived from the experiments and compared with the results of theoretical calculations. The bonding and geometry of the Cu^{2+} polyhedra is strongly influenced by the Jahn–Teller effect.

Acknowledgment. One of the authors gratefully acknowledges the cooperation with Dr. G. F. Kokoszka (NATO grant) with respect to V-band EPR spectroscopy and line-shape effects.

Registry No. $K_2Cd_2(NO_2)_6$, 98542-08-6; $Rb_2Cd_2(NO_2)_6$, 85565-57-7; $Tl_2Cd_2(NO_2)_6$, 37956-94-8; $Cs_2Cd_2(NO_2)_6$, 37956-95-9; $Tl_2Hg_2(NO_2)_6$, 98542-09-7; $Cs_2Hg_2(NO_2)_6$, 37956-96-0; $Cs_2PdHg(NO_2)_6$, 98542-10-0; Cu^{2+}, 15158-11-9.

Contribution from the Department of Chemistry,
The University of Chicago, Chicago, Illinois 60637

Energetic Description of Solids in Terms of Small Fragments

JEREMY K. BURDETT* and DUANE C. CANEVA

Received January 9, 1985

The following inorganic solids were studied, with use of both tight-binding band structure computations on the crystal and molecular orbital calculations on small fragments torn from the crystal lattice: α-BeO, cooperite, $PdCl_2$, β-tridymite, β-quartz, stishovite, and silica-w. Not only are the demands of the local angular geometry of both anion and cation important in determining the details of the structure but the energetics of the anionic matrix play an important role also. In all of these systems it appears that the repulsions between the closed shells of electrons associated with the anions are close to being minimized in the observed structure, subject to the constraint of constant anion–cation distance. Comments are made on the validity of geometrical and energetic data obtained from calculations on small molecular units torn from the lattice, which do not have the same stoichiometry as the solid.

Introduction

When we attempt to understand the factors that determine crystal structure with the aid of numerical calculations of one type or another, the problem that we invariably face is how to sort out from the numerology concepts and ideas that are useful in a qualitative as well as quantitative sense. In general, we feel particularly happy if we can attribute stability to geometrical features that involve small groups of atoms: in other words, focus on rather local effects. Bland statements of the type that structure A is more stable than structure B because it has a larger Madelung constant or lower total energy calculated via some quantum-mechanical method are less attractive in this regard.

A useful approach in the past decade or so has been the study of the energetics of relevant structural units[1-4] torn from the crystal lattice whose dangling bonds have been sealed with either electrons or hydrogen atoms. So, for example, studies of SiO_4^{4-}, $(SiH_3)_2O$, and analogous molecules where silicon has been replaced by aluminum or phosphorus have been invaluable in casting light on structural features of silicate materials.[2,3] In this paper we compare results obtained for a variety of systems using both molecular orbital calculations on small fragments and tight-binding calculations on crystalline structures. Exactly the same method and parameters are used in both areas (the extended Hückel ansatz), and so we hope not only to understand why these systems adopt the structures they do but also to investigate the validity of such local cluster calculations and see how good such one-electron methods are in reproducing the observed geometrical details of extended solid-state arrays. Although we shall use the terms anion and cation in this paper to represent respectively the more electropositive and electronegative atoms of the solid and will in fact only consider systems with a significant electronegativity difference between the constituents, we do not intend this usage to imply dominance of ionic interactions in bonding. In fact, we use an orbital picture of these solids where such Coulombic forces are not explicitly included.

α-Beryllia (BeO)

The lowest energy polymorph of BeO has the wurtzite structure. Elsewhere we have investigated[1a] the factors that locate this arrangement as the one of lowest energy, rather than another way of filling of the tetrahedral holes in the structure. The space group of the structure is $P6_3mc$ with the Be atoms in 2(a): (0, 0, u_1; $^1/_3$, $^2/_3$, $^1/_2 + u_1$) and the O atoms in 2(a) (0, 0, u_2; etc.) (Figure 1). There are therefore three degrees of freedom in this structure, the crystallographic parameters a, c and $u_1 - u_2$ (u). Fixing the axial (parallel to z) and basal Be–O distances (l) leads to one variable (u) so that

$$\gamma^2 = \frac{4}{12u - 3} \tag{1}$$

where $\gamma = c/a$, the axial ratio. The volume is given by

$$V = \frac{l^3(u - \frac{1}{4})}{2u^3} \tag{2}$$

The maximum volume subject to this constraint occurs at $u = {}^3/_8$. Four sets of calculations were performed in which u was varied: (i) a band structure computation for the BeO crystal (see the Appendix for details.); (ii) a calculation, similar to (i) but where the Be atoms were missing and the lattice was considered as being made up of oxide anions; (iii) local geometry calculations for BeO_4^{6-} ions; (iv) local geometry calculations for OBe_4^{6+} ions. In the last two calculations interactions between the ligands were "switched off" so that the results measure the effect of geometry variation on local anion–cation interactions and the effect of the anion lattice is not double counted. At $u = {}^3/_8$ several geometrical features are in coincidence. First the oxide ions are in hexagonal eutaxy. (We use O'Keeffe's terminology[5,6] here to describe the arrangement of ions whose centers are located at the centers of hard spheres in a closest packing. In this way we remove from discussion the nebulous concept of "ionic size".) Second, both oxygen and beryllium geometries are exactly tetrahedral. For real molecules with such electronic configurations this of course is the geometry expected. Figure 2 shows the energetics associated with the set of calculations described above, and also an estimate of the total energy variation with u as a weighted sum of the indi-

---

(1) (a) Burdett, J. K.; McLarnan, T. J. *Am. Mineral.* **1984**, *69*, 601. (b) Burdett, J. K.; McLarnan, T. J. *J. Chem. Phys.* **1981**, *75*, 7554.

(2) (a) O'Keeffe, M., Navrotsky, A., Ed. "The Structures of Complex Solids"; Academic Press: New York, 1981. (b) Gibbs, G. V. In ref 2a.

(3) (a) Lager, G. A.; Gibbs, G. V. *Am. Mineral.* **1973**, *58*, 756. (b) O'Keeffe, M.; Gibbs, G. V. *J. Chem. Phys.* **1984**, *81*, 876. (c) Gibbs, G. V. *Am. Mineral.* **1982**, *67*, 421.

(4) Tossell, J. A. *Trans. Am. Crystallogr. Assoc.* **1979**, *15*, 47.

(5) O'Keeffe, M. *Acta Crystallogr., Sect. A: Cryst. Phys., Diffr., Theor. Gen. Crystallogr.* **1977**, *A33*, 924.

(6) O'Keeffe, M. In ref 2a.

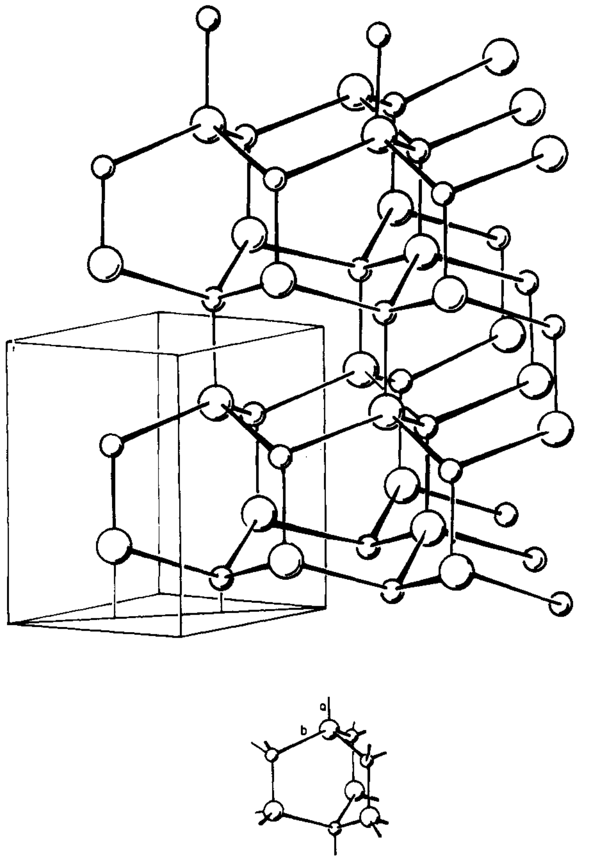

Figure 1. The wurtzite structure adopted by α-BeO.

vidual calculations (ii–iv). Qualitatively the agreement between the computed total energy and that estimated in this way is fine, but quantitatively it is not exact. Among other things we have assumed complete charge transfer to oxygen (and treated it as O^{2-} in (ii)) whereas such transfer is not complete in (i). The charge calculated via a population analysis of the band structure computation of (i) is −1.1 electrons per oxygen atom. Thus the magnitude of the variations in calculation ii is an overestimate. Notice, however, that in spite of this the estimate of the energy changes in curve d shows a smaller variation with u than does curve a. The reasons for the adoption of the wurtzite structure at this particular value of u are that it corresponds concurrently with an energy minimum for both the oxide lattice and the local arrangements of the ions. Notice that the former occurs at the maximum volume geometry.

Most wurtzites do not in fact have γ ratios or u parameters exactly equal to the values corresponding to hexagonal eutaxy.[7–9] There is no symmetry requirement for the one axial (parallel to z) and three basal linkages around each center to be equal or the three angles linking axial and basal linkages to be the same as the three angles associated with the basal linkages. (The site symmetry is C_{3v}.) A distortion away from the ideal geometry via changes in bond lengths and/or angles is then a possibility. For electronegativity differences less than a certain critical value, γ values greater than and u values smaller than ideal are found.[9] These correspond to materials where, although the wurtzite modification is known, the structure is more stable in the cubic sphalerite structure. For electronegativity differences greater than this critical value (corresponding to more "ionic" systems) the converse is true. The examples that fall into this latter category exhibit the wurtzite, or sometimes the rock salt structure, as the most stable variant. (It is worth pointing out at this stage that although the γ ratio for many wurtzites is known, the u parameter has only been determined in a handful of cases.) Several distortion possibilities arise, but since one of the weakest points of the one-electron model we are using is the accurate mimicking of bond length changes, we shall only consider distortions that keep the average Be–O distance constant. The mode that allows no angular geometry change around either center is achieved by keeping $\gamma(^1/_2 - u)$ constant during the distortion and for $\gamma > \gamma_{\text{ideal}}$ corresponds to lengthening the axial bond at the expense of the basal ones. The distortion that corresponds to the observed behavior for the rather small collection of wurtzites where both u and γ have been experimentally determined is described by either a linear (eq 3) or hyperbolic relationship (eq 4). Here the angular geometry

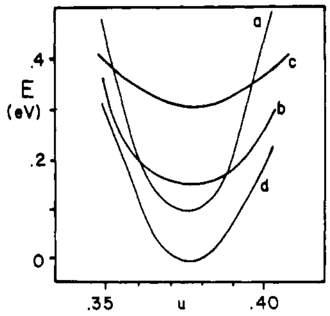

Figure 2. Energetic variation with u for wurtzite BeO: (a) tight-binding calculation on BeO; (b) tight-binding calculation on the oxide ion lattice; (c) molecular orbital calculations on BeO_4^{6-} and OBe_4^{6+} fragments, giving the sum of the energetic variations at both atoms; (d) estimate of (a) by a weighted sum of the contributions of (b) and (c). The absolute energies associated with the four sets of results are obviously very different. Thus on this and on similar figures in this paper we have shown relative energy changes on distortion and vertically shifted the location of the different curves for cosmetic purposes. Relative energies are for two formula units.

$$u = u_{\text{ideal}} + \text{const}(\gamma - \gamma_{\text{ideal}}) \tag{3}$$

$$\gamma u = \text{const} \tag{4}$$

changes too and for $\gamma > \gamma_{\text{ideal}}$ corresponds to a lengthening of the basal linkages at the expense of the axial one. A population analysis of the tight-binding orbitals at the ideal geometry for BeO gives no clues as to the preferred distortion route. Using the parameters described in the Appendix, we find a negligible difference in the overlap populations for the two symmetry-inequivalent linkages. An energy minimum is found at the undistorted geometry for distortion along either pathway where the average anion–cation distance is kept constant. This geometry is also the energy minimum found for the collection of oxide ions alone. However, all of these potential energy surfaces are extremely soft with this constant average bond length model. Clearly the orbital model does not pick up the distortion to smaller γ values for this AX system with a large A–X electronegativity difference. A calculation performed on BeO in the sphalerite modification with the same Be–O distance shows a very small stabilization (~0.2 kcal/mol) relative to the wurtzite modification.

We have performed similar calculations on the all-carbon system, which as diamond adopts the cubic (degenerate sphalerite) structure, although the degenerate wurtzite arrangement is known as lonsdaleite. Here the overlap populations for the symmetry-inequivalent linkages in the hexagonal structure are slightly different (**1**) and predict longer axial than basal linkages. Figure 3 shows the energetics associated with the three distortion pathways noted above. Interestingly, distortions to structures with γ values greater than ideal are calculated to be energetically

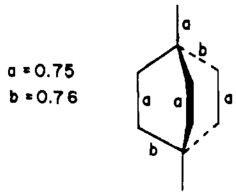

1

---

(7) Keffer, F.; Portis, A. M. *J. Chem. Phys.* **1957**, *27*, 675.
(8) Lawaetz, P. *Phys. Rev. B: Solid State* **1972**, *10*, 4039.
(9) Bloch, A. N.; Schatteman, G. C. In ref 2a.

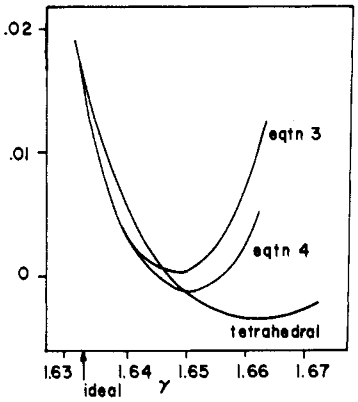

Figure 3. Energetic variation for non-bond-length-conserving distortions in hexagonal diamond. The bottom curve corresponds to the distortion that preserves the regular tetrahedral geometry about each atom.

favored for all models. This is what is found experimentally, and indeed we compute the energetically preferred pathway to be the one that leads to shorter basal and longer axial linkages as predicted from **1**. However, the energy changes involved are are not large and the distortions that lead to bond length changes in the opposite sense are close in energy. It would be of great interest to have a *u* value for lonsdaleite[10] to see if the relative bond lengths are indeed in accord with **1**. A calculation on cubic diamond using the same internuclear separation as for the hexagonal form showed an energy of stabilization of the cubic form of 1.9 kcal/C_2. We have also performed calculations on a "BeO" system where the atomic orbital energies correspond to a much more electronegative metal species. (We used H_{ii} values for the 2s and 2p orbitals of −16.0 and −9.0 eV.) Here, as in BeO itself, the differences in the overlap populations associated with the symmetry-inequivalent linkages are tiny, but the energetics of distortion predict movement away from the symmetrical geometry toward higher γ values. A calculation on the cubic structure with these parameters showed a stabilization of this structure of 0.6 kcal/mol relative to the hexagonal variant. This is somewhat larger than for the "real" BeO system described earlier. So, as the electronegativity difference between the constituents of the structure decreases, the calculations mimic experiment in two ways. First, the cubic structure becomes increasingly more stable relative to the hexagonal alternative. This may be understood in terms of concepts from molecular chemistry. The six-membered rings in the sphalerite structure are all of the chair type. In wurtzite half of the rings are chairs, but the other half are in the less energetically favored boat conformation. The energetic discrepancy between the two will increase as the electronegativity difference between A and X decreases.[11] Second, a distortion toward a hexagonal structure with a γ value larger than ideal becomes increasingly favored. What we do not find is any stabilization of a wurtzite with a γ ratio less than ideal, the experimental observation for all systems where the wurtzite form is known to be the more stable polymorph. The orbitally based tight-binding calculations appear then to be a useful model for the more covalent materials but do not seem to be as good in getting the details of the structure correct for more ionic systems. Although this result could perhaps have been anticipated, we have used BeO as a model compound elsewhere[1a] to study Pauling's rules via orbitally based tight-binding calculations. BeO is "covalent" enough to have provided useful results in that study. It is worth pointing out that the energetic changes involved for these systems with large electronegativity differences are very small indeed when evaluated by our methods and that the state of affairs could change dramatically if the restriction of constant average bond length were relaxed. This restriction was imposed since the extended Hückel model invariably mimics the energetics associated with bond length changes rather poorly. Notice that the calculated energetics of the more "ionic" structures parallel those of the oxide lattice. It could perhaps be argued that our failure to reproduce the observed structures of wurtzites with $\gamma < \gamma_{\mathrm{ideal}}$ is due to a poor approximation to the O–O pair potential. We have encountered similar problems elsewhere[12] in getting the finer details of the rutile structure correct. Hyde and O'Keeffe[13] have studied this problem using their extension of the Bartell–Glidewell nonbonded repulsion ideas and conclude that the details of the geometries of systems with $\gamma < \gamma_{\mathrm{ideal}}$ are determined by nonbonded repulsions between the cations. This problem is one that should be reinvestigated with use of a theoretical model that numerically is more accurate than ours.

Cooperite (PtS)

The structures of PtS, PdO, and PtO (**2**) have the space group $P4_2/mmc$ with the metal atoms in 2(c) (0, $^1/_2$, 0; $^1/_2$, 0, $^1/_2$) and the nonmetals in 2(e) ($\pm$(0, 0, $^1/_4$). Fixing the anion–cation distance (l) allows the structure to be described by one variable (the axial ratio $c/a = \gamma$), and the volume is given by

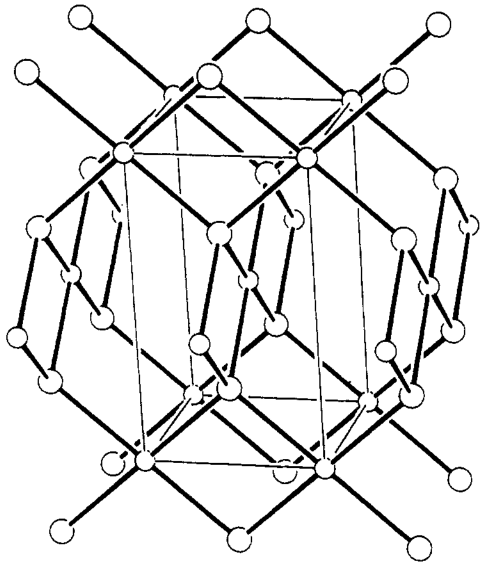

2

$$V^2 = 4096\gamma^2 \frac{l^6}{(4+\gamma^2)^3} \qquad (5)$$

The observed value of γ is 1.76 (for PtS and PtO) and 1.75 for PdO. Geometrically the system may be described as being made up of an approximately eutactic array of oxide ions, where in PdO each Pd is four-coordinated by oxygen in an approximate square-planar arrangement and each oxygen is approximately tetrahedrally coordinated by Pd atoms. At $\gamma = 2$ the Pd is exactly square planar and at $\gamma = 2^{1/2}$ the oxygen atoms are exactly tetrahedral and the metal atoms in cubic eutaxy. The second case corresponds then exactly to a defect fluorite structure. The maximum volume of the structure also occurs at $\gamma = 2^{1/2}$.[14]

Figure 4 shows the results of four sets of calculations for PdO analogous to the ones performed for BeO above. An energy minimum is calculated close to that found experimentally. Notice that, as expected, the energy variation associated with the local metal geometry has a minimum at $\gamma = 2$ and that associated with the oxygen geometry has a minimum at $\gamma = 2^{1/2}$. Notice too, however, the energetically important contribution from the repulsions of the closed-shell oxides. These do not find a minimum at the maximum volume structure but a shallow minimum at much higher γ and close to $\gamma = 2$. This result is understandable since at $\gamma = 2$ all close O–O distances (around the square) are equal. At $\gamma = 2^{1/2}$, where a rectangular coordination is found, there are

---

(10) It is perhaps surprising that so many of these wurtzites have not been examined in sufficient detail for this parameter to have been determined.

(11) Burdett, J. K. *J. Am. Chem. Soc.* **1980**, *102*, 450.

(12) Burdett, J. K. *Inorg. Chem.* **1985**, *24*, 2244.

(13) O'Keeffe, M.; Hyde, B. G. *Acta Crystallogr., Sect. B: Struct. Crystallogr. Cryst. Chem.* **1978**, *B34*, 3519.

(14) These comments correct errors concerning this structure in ref 5.

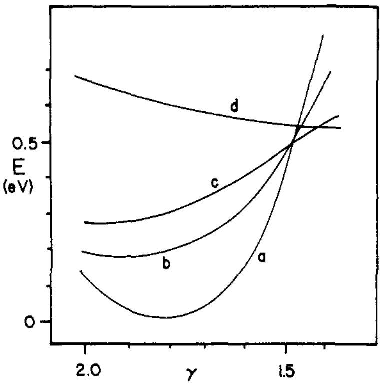

Figure 4. Energetic contributors to the distortion of the cooperite structure as a function of the axial ratio $c/a = \gamma$: (a) tight-binding calculation on a PdO crystal; (b) tight-binding calculation on the oxide lattice; (c) molecular orbital calculation on a PdO_4^{6-} fragment; (d) molecular orbital calculation on a OPd_4^{6+} fragment. Relative energies are for two formula units.

two short and two long distances. From the curvature of a typical[12] O–O repulsion curve (**3**) it is clear that the former is of lower energy.

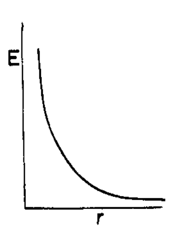

3

The balance of the energetics associated with local metal and oxygen coordination has long been recognized[7] as being important in fixing the details of this structure. Here we have pointed out the effect of the anion matrix itself. Energetically its contribution is certainly overestimated for reasons we have mentioned above, but the balance of three and not two geometrical effects is the one indicated by the calculations. The idea of a "matrix effect" in determining the details of structures has been examined in some detail by Corbett[15] for several early-transition-metal-containing species. We have been able to assess numerically[16] the distortion of the Chevrel phases from the idealized to the observed structure, a structural change with a strong matrix component. In all of the examples described in this paper we will see that energetically it is a very important effect.

$PdCl_2$

This structure is orthorhombic, space group *Pnnm*, with the metal atoms in 2(b) (0, 0, $^1/_2$; $^1/_2$, $^1/_2$, 0) and the halogens in 4(g) ($\pm$(u, v, 0; u + $^1/_2$, $^1/_2 - v$, $^1/_2$)). $PtCl_2$ is isostructural. Geometrically (**4**) it may be described as chains of edge-sharing $PdCl_2$ units, containing approximately square-planar metal atoms, running parallel to z. With the constraint of constant Pd–Cl distance there are still several variables to completely describe the structure. However, varying θ of **5**, within a constant bond length approximation, and keeping u and v constant led to energy changes that were very close to those found by variation of θ within a single $PdCl_2$ chain. The energetics of Figure 5 for single one-dimensional chains of $PdCl_2$ are very simple to understand. The geometry appears to be dominated by the energetics associated with the anion array. The square geometry around the metal is not energetically favorable since there are twice as many anion–anion repulsions parallel to the chain than perpendicular to it. The favored matrix geometry should then be for an angle $\theta < 45°$ as is indeed found. Notice from Figure 5 that the energetic effect of local anion or cation geometric variations is small by comparison.

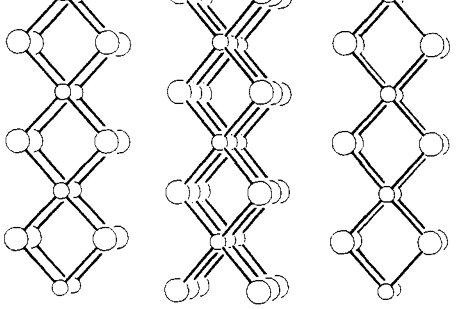

4

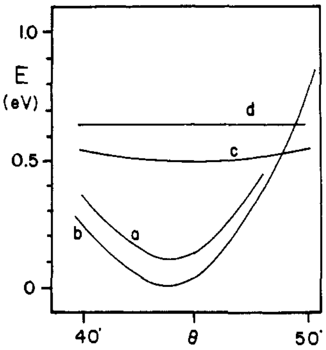

Figure 5. Energetics of distortion of a single chain of the $PdCl_2$ structure as a function of θ of **5**: (a) one-dimensional tight-binding calculation on a single $PdCl_2$ chain; (b) tight-binding calculation on the chloride ion matrix; (c) molecular orbital calculation on a $PdCl_4^{2-}$ fragment; (d) molecular orbital calculation on a $ClPd_4^{2+}$ fragment. Relative energies are for two formula units.

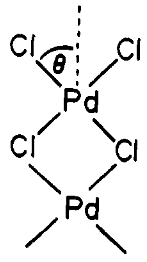

5

β-Tridymite (SiO_2)

This perhaps hypothetical structure is essentially the degenerate α-BeO arrangement but with spacers between the tetrahedrally coordinated atoms. Formally in space group *P*6/*mmc*, the silicon atoms occupy 4(f) ($\pm$($^1/_3$, $^2/_3$, u; $^2/_3$, $^1/_3$, u + $^1/_2$)) and the oxygen atoms occupy 2(c) ($\pm$($^1/_3$, $^2/_3$, $^1/_4$)) and 6(g) ($^1/_2$, 0, $^1/_2$; 0, $^1/_2$, $^1/_2$; $^1/_2$, $^1/_2$, 0; $^1/_2$, 0, 0; 0, $^1/_2$, 0; $^1/_2$, $^1/_2$, $^1/_2$). Fixing the lengths of the axial and basal Si–O linkages enables the structure to be described in terms of one variable (u). During variation of u the oxygen coordination remains linear. All that changes locally is the angular geometry of the silicon atom in a way analogous to that of either atom in BeO above. At $u = {}^7/_{16}$ this geometry is tetrahedral. As a function of u the volume of the structure is given by

$$V = 6(3^{1/2})l^3\frac{(u/2 - 3/16)}{(u - 1/4)^3} \qquad (6)$$

which has a maximum at $u = {}^7/_{16}$. Figure 6 shows the results of three sets of calculations as a function of u: (i) band structure computations on crystalline SiO_2; (ii) band structure computations on the oxide ion lattice of such a crystal; (iii) calculations on SiO_4^{4-} molecules.

There are clear similarities between the conclusions we draw for the idealized α-BeO and β-tridymite structures. The lowest

---

(15) Corbett, J. D. *J. Solid State Chem.* **1981**, *39*, 56; **1981**, *37*, 335.
(16) Burdett, J. K.; Lin, J.-H. *Inorg. Chem.* **1982**, *21*, 5.

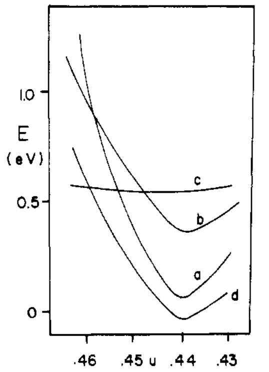

Figure 6. Energetic contributors for the distortion of the β-tridymite structure as a function of u: (a) tight-binding calculation on SiO_2; (b) tight-binding calculation on the oxide ion lattice; (c) molecular orbital calculation on an SiO_4^{4-} fragment; (d) estimate of (a) using a weighted sum of (b)–(d). Relative energies are for four formula units.

Table I

	u	γ	Si–O–Si angle
obsd	0.2091	1.0925	153.1 (2)
calcd	0.221	1.1	154.2
O^{2-} ions only	0.212	1.1	
$Si_2O_7^{6-}$ unit	0.220	1.1	
max vol	0.250	1.061	

energy arrangement is the one that, given a fixed cation-oxygen distance (l), minimizes the repulsions between the closed-shell O^{2-} ions (in these cases maximizes the volume subject to such a constraint), and also satisfies the tetrahedral coordination about the beryllium and oxygen in BeO and the silicon in SiO_2. This viewpoint is little different from that of O'Keeffe,[7] who implicitly ascribed the stability of the maximum volume structure to electrostatic effects. In our tight-binding calculations the energetics of the oxide lattice are controlled by the overlap repulsions of closed shells of oxide ions.

β-Quartz

There has recently been a high-quality neutron diffraction study of the high- and low-temperature forms of quartz.[17] The best *ordered* model for β-quartz corresponds to a structure with space group $P6_222$ with the silicon atoms in 3(c) ($^1/_2$, 0, 0; 0, $^1/_2$, $^2/_3$; $^1/_2$, $^1/_2$, $^1/_3$) and the oxygen atoms in 6(j) (u, $2u$, $^1/_2$; $2u$, u, $^1/_6$; $\bar{u}$, u, $^5/_6$; $\bar{u}$, $2\bar{u}$, $^1/_2$; $2\bar{u}$, $\bar{u}$, $^1/_6$; u, $\bar{u}$, $^5/_6$). A model where both oxygen and silicon are disordered about these sites fits the data best.) Fixing the Si–O distance equal to $l = 1.62$ Å leads to two degrees of freedom for this structure, which we will define as γ ($=c/a$) and the parameter u. The volume is given by

$$V^2 = 9\frac{\gamma^2}{16}\,\frac{1}{(3u^2 - 3u/2 + 1/4 + (\gamma/6)^2)^3} \qquad (7)$$

We have performed tight-binding calculations on the crystal and calculated the energy as a function of u and γ. The result is a well-defined valley along the direction defined by $\gamma = 1.1$. Figure 7 shows a slice through the potential energy surface along this valley. The calculated energy minimum for SiO_2 (Table I) compares very favorably with the observed values of u, γ, and the Si–O–Si angle. Figure 7 also shows a curve for the energetic variation with u of the oxide ions alone of such an array. Notice that the calculated minimum energy geometry for the SiO_2 crystal is close to that found in this calculation. The maximum volume structure, although close by, does not correspond exactly to this arrangement. If we insist on regular tetrahedra for this structure and keep all the Si–O distances constant, then there are no free parameters for the structure at all. ($\gamma = 1.098$, $u = 0.2113$, and the O–Si–O angle is fixed at 155.6°). Thus the structures calculated to be lowest in energy are those containing close to regular tetrahedra. As far as the geometric details of the oxide lattice are concerned, it seems to be immaterial as to whether the tetrahedra are actually occupied!

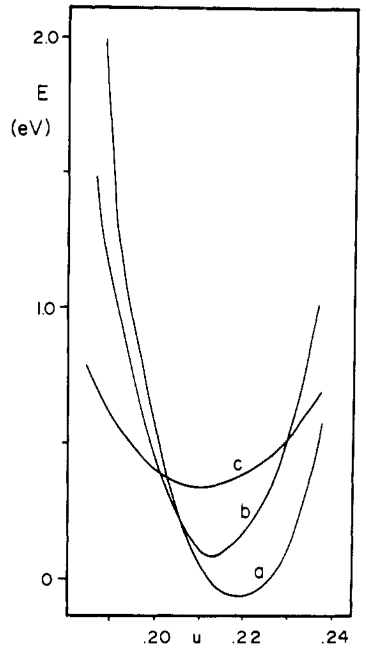

Figure 7. A slice through the potential energy surface, $E(u,\gamma)$ for β-quartz at $\gamma = 1.1$: (a) tight-binding calculation on SiO_2; (b) same as (a) but with all interaction integrals between orbitals separated by more than 3 Å set to zero (removes all through-space Si–Si interactions); (c) tight-binding calculation on the oxide ion lattice alone. Curve c is indistinguishable from one with a 3-Å cutoff. Relative energies are for four formula units.

Hyde and O'Keeffe have argued[18] for strong control of the geometry of such systems by through-space repulsions between the silicon atoms. (This is the Bartell–Glidewell[19] hard-sphere approach applied to solids.) Such repulsions have been suggested to be the reason for the opening up of the Si–O–Si angle (Table I) from the the values close to the tetrahedral angles normally found in oxygen halides and hydrides. We can get some feel for the effect of such interactions on our model by switching off all interactions between the silicon atoms in the calculation. In practice we did this by setting to zero all overlap integrals between orbitals less than 3 Å apart. These results are also shown in Figure 7. Although the shapes of the two curves from the tight-binding calculations on the SiO_2 crystal are virtually identical, the effect of including the Si–Si interactions has been to open up the Si–O–Si angle by about 3°. Also, not evident from the plot is that the total energy is substantially lower when these interactions are dropped. By contrast, the plot found for the oxide lattice alone by employing this 3-Å cutoff is indistinguishable from that shown in Figure 7. Thus we conclude that direct Si–Si interactions are indeed repulsive (as also indicated by a negative overlap population between these atoms) and are responsible for an opening up of the angle at oxygen of a few degrees. Introduction of the silicon atoms into the oxide lattice also has the effect of stiffening the framework, as evident from the different curvature of the plots (b) and (c) of Figure 7.

It is interesting too to examine the geometry predicted via these simple calculations for an isolated $Si_2O_7^{6-}$ unit, a molecular fragment similar to the $SiO(OH)_6$ molecule, which has often been used[3,20] to mimic the energetics of silicate materials in general. Curve a of Figure 8 shows how the energy of such a molecule,

---

(17) Wright, A. F.; Lehmann, M. S. *J. Solid State Chem.* **1981**, *36*, 371.

(18) O'Keeffe, M.; Hyde, B. G. *Acta Crystallogr., Sect. B: Struct. Crystallogr. Cryst. Chem.* **1976**, *B34*, 2923.

(19) (a) Bartell, L. S. *J. Chem. Phys.* **1960**, *45*, 754. (b) Bartell, L. S.; Plato, V. *J. Am. Chem. Soc.* **1973**, *95*, 3097. (c) Bartell, L. S. *Croat. Chem. Acta* **1984**, *57*, 927. (d) Glidewell, C. G. *Inorg. Chim. Acta* **1975**, *12*, 219.

(20) Gibbs, G. V.; Newton, M. D. In ref 2a.

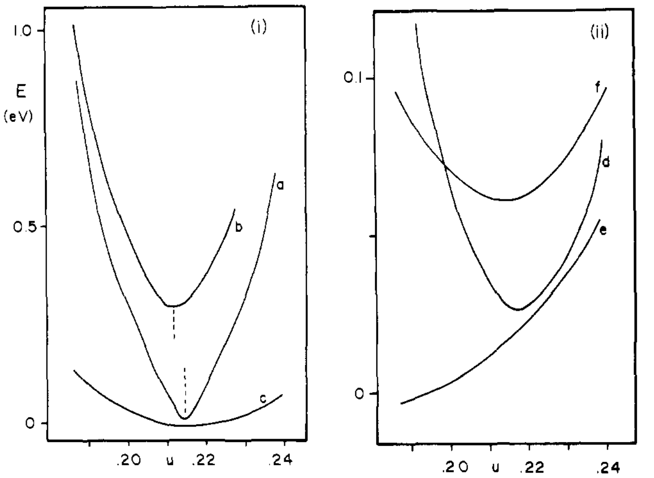

Figure 8. (i) Molecular orbital calculations on an $Si_2O_7^{6-}$ fragment constrained to adopt the geometry found for this unit in the crystal. Three curves showing the effect of dropping the interaction integrals between various sets of atoms: (a) full molecular orbital calculation on $Si_2O_7^{6-}$; (b) calculation with Si–Si interactions dropped; (c) calculation with all nonbonded interactions dropped. (ii) Three additional curves: (d) the same curve as (c) above; (e) calculation on $Si_2O_7^{6-}$ but with preservation of an exactly tetrahedral geometry at each silicon atom; (f) calculation on an SiO_4^{4-} unit. The energy curve here is multiplied by two for comparison with (e).

constrained to follow the geometry found for this unit in the crystal, changes as the value of u is varied. A minimum, close to that found in the full crystalline calculation, is found. Our result is an interesting one since bending an isolated $Si_2O_7^{6-}$ unit at the oxygen atom while freezing the local geometry around each silicon atom leads to the calculation of a soft potential energy surface with an energy minimum at the linear Si–O–Si geometry (curve e). Elsewhere we have argued[12,21] that this is due to strong π-bonding between silicon and bridging oxygen atoms, a consequence of the SiO_3 unit being a good π-acceptor. We have proposed a similar explanation for the stabilization of planar three-coordinate oxygen in rutile[12] and square-planar oxygen in NbO.[22] Clearly our calculational method overestimates such a stabilization in the present case and does not reproduce the 1–2 kcal/$Si_2O_7^{6-}$ stabilization (the exact value dependent upon Si–O distance) expected for this unit by comparison with ab initio results on disiloxane.[20] We can investigate the importance of nonbonded repulsions between the silicon atoms on our model by employing the same trick described above and dropping from the calculation interaction integrals between atoms less than a certain distance apart. When the geometry of the end groups is kept fixed, there is little difference in the result. A linear molecule is predicted irrespective of whether silicon–silicon interactions are included or not. Therefore, on our model there is no evidence for the opening up of the O–Si–O angle by Si–Si nonbonded interactions. The results for the molecular fragments which geometrically follow the crystalline solid are collected together in Figure 8i. When the interactions between the nonbonded silicon atoms are eliminated, the result, as in the full crystal calculation, is an energy lowering. There is also a shift of the equilibrium Si–O–Si angle of a few degrees to a larger value associated with virtually no change in the shape of the potential energy curve. A dramatic effect is seen when the interactions between the oxygen atoms are switched off. The result is a much flatter surface than before, once again emphasizing the dominance of the energetics by anion–anion repulsions. Notice the similarities between the plots of Figure 7 and Figure 8i.

Why are the calculations on the rigid and nonrigid $Si_2O_7^{6-}$ molecules of Figure 8ii so different? The answer is forthcoming when we examine the curve for an isolated SiO_4^{4-} unit, shown in curve f. As the molecule moves away from the regular tetrahedral geometry, so the energy increases. The overall effect is a coupling between the energetic preferences at oxygen and silicon. This state of affairs is described pictorially in Figure 9.

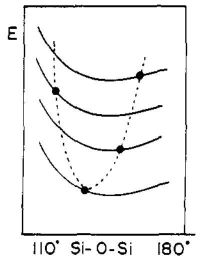

Figure 9. Schematic, showing a set of potential energy curves corresponding to bending an isolated $Si_2O_7^{6-}$ unit at the oxygen atom while keeping the local silicon geometry fixed. Each curve corresponds to a different geometry at silicon. The dashed line shows the traverse made by changing the u coordinate as in Figure 7.

From Figure 8ii we would say that the reason for the adoption of the β-quartz structure with this value of u is because here the silicon atom is in an energetically comfortable tetrahedral geometry. From Figures 7 and 8i, however, it is clear that energetically the most important contributions come from the minimization of the energetics of the anionic lattice along with a contribution from repulsions between the silicon atoms. The two different viewpoints may be unified since the angular geometry at silicon is strongly influenced by the repulsions between the oxide ligands. In this paper, in assessing local geometry effects, we have dropped ligand–ligand interactions, so as not to double-count their effect when looking at the energetics of the oxide lattice. In fact, of course, the two are inseparable; the factors controlling the angular geometry of a molecule include both the repulsions of the ligands and the energetics (orbital preferences) of central-atom–ligand interaction. This difference in the scale of the energy changes depicted in Figures 7 and 8 is however quite important. Of special interest is the difference in magnitude of the distortion energy for the $Si_2O_7^{6-}$ molecule and that of the crystal calculation. A part of the discrepancy arises from the fact that Si_2O_7 and (for the crystal with three formula units per unit cell) Si_3O_9 stoichiometries are being compared. A major conclusion must be, however, that the use of numerical data from calculations on molecules to model solids may often be in error. This arises in part because the terminal atoms of the cluster chosen are in a very different environment in the solid, being surrounded by energetically important close contacts. This comment is also applicable to calculations where the Si–O–Si angle is varied while a frozen terminal unit geometry is kept, since here interactions of the bridging oxygen atom with other anions (numerically important in our calculations) have been neglected.

Orthorhombic Silica and Stishovite

Elsewhere[12] we have examined the structure of stishovite (SiO_2 in the rutile arrangement) and shown how the energetics can be described as a sum of matrix and local effects, with probably some contribution from repulsions between the silicon atoms. A feature of this structure is the set of infinite chains of edge-sharing octahedra running parallel to the z axis (**6**). These chains are linked to each other to produce a three-dimensional framework structure. The structure of orthorhombic silica (silica-w) has been reported to have a chainlike structure, but made up of isolated chains of edge-sharing tetrahedrally based units (**7**). SiS_2 and $BeCl_2$ are isostructural.[23] As a building block of the polymeric material

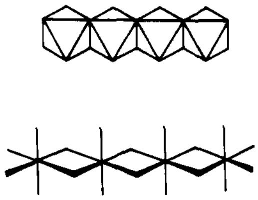

6

---

[21] Albright, T. A.; Burdett, J. K.; Whangbo, M.-H. "Orbital Interactions in Chemistry"; Wiley: New York, 1985.

[22] Burdett, J. K.; Hughbanks, T. *J. Am. Chem. Soc.* **1984**, *106*, 3101.

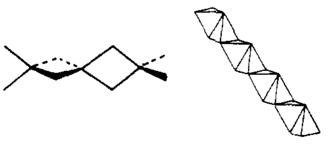

7

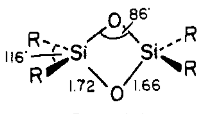

R = Mesityl

8

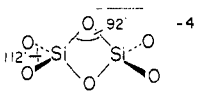

9

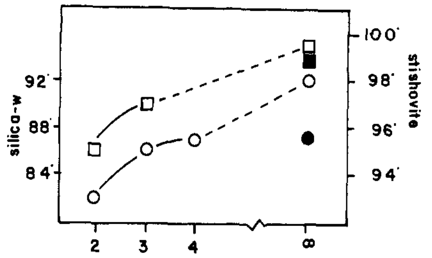

Figure 10. The computed Si–O–Si angle in a single chain of stishovite (squares) and a single chain of silica-w (circles), as a function of the number of atoms included in the structural unit used to mimic the infinite solid. The result labeled with an infinity sign represents that obtained via a band structure calculation on the solid. The solid symbols represent the experimentally determined values.

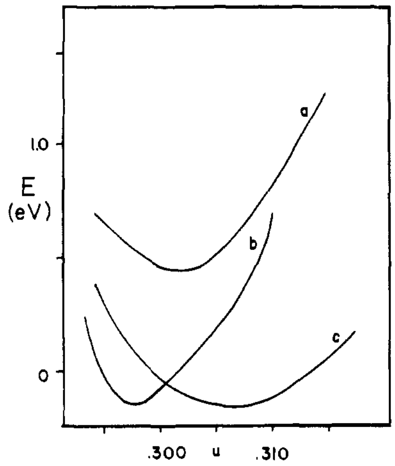

Figure 11. Potential energy changes associated with changing the Si–O–Si angle in stishovite by variation of the coordinate *u* of the rutile arrangement. The results are shown for (a) the infinite one-dimensional chain of stishovite, (b) a two silicon atom unit, $Si_2O_{10}^{8-}$, to mimic this structure, and (c) the same case as for (b) but with the interaction integrals between the orbitals located on both pairs of terminal oxygen atoms set to zero. Internal and external O–Si–O angles are kept equal in the distortions leading to curves b and c.

the molecule **8** has recently been characterized[24] crystallographically. Of interest to us in this paper is how well the geometry and dynamical properties of the infinite solid are mimicked by calculations on small fragments. Figure 10 shows how the angle at oxygen in the lowest energy computed geometry depends upon the number of atoms in the chain for the two systems. The calculated minimum for the stishovite chain via a band structure calculation is close to that observed experimentally from a high-quality single-crystal X-ray determination.[25] The Si–O distance (1.77 Å) used in our calculation[12] is the average distance in the full structure. The Si–O distance within the chain in the crystal is 1.757 Å. Use of this slightly shorter distance in the calculation gives a computed bond angle at oxygen exactly where it is found experimentally. The angle at oxygen from a powder pattern study of silica-w is 87.2°.[26] This is somewhat smaller than that from our calculation.[27] Notably in both cases the computed angle changes rather dramatically with the size of the unit studied. A clue to the reason behind this observation lies in the values of the angles we find for the energy-minimized structure of the $Si_2O_6^{4-}$ unit shown in **9**. O'Keeffe and Gibbs[3b] find an angle at oxygen of 92.8° (with an Si–O distance of 1.670 Å) from an ab initio calculation on $Si_2O_2(OH)_4$. As the external angle opens up, so the angle at oxygen approaches the value found for the infinite case. Clearly a dominant energetic feature of these structures is the repulsion between the oxygen atoms of the bridge. In all of these small fragments chosen to represent the infinite solid, there are more close O–O contacts per silicon atom than in the infinite unit. It is not then unexpected that the computed angle at oxygen is smaller for the small fragments than the value found for the infinite chain. Using our molecular orbital method, we can test this hypothesis since the interactions between the end pairs of oxygen atoms may be switched off. The result is shown in Figure 11 for the stishovite case and shows a striking change in the calculated minimum energy geometry. The equilibrium geometry of these systems is set by strong O–O repulsions (a matrix effect), and accurate mimicking of such interactions is clearly vital for the correct geometry to be obtained. Switching off all the interactions between the orbitals located on the terminal atoms overshoots the value for the infinite chain, since now there is only one close O–O contact per Si_2 unit. (Interestingly the ab initio calculation of ref 25a, which used the $Si_2F_8(OH)_2$ molecule as a model for the stishovite chain, also gave an angle at oxygen that was too high.) Notice too, that in addition to the shift in the minimum energy angle, the bending potential becomes softer when these interactions are dropped. When estimating the energy of the crystalline materials via ab initio molecular orbital calculations on fragments, it would then appear essential to include the correct number of close O–O contacts per formula unit. The recent assessment of O'Keeffe and Gibbs[3b] of the stability of silica-w, which used the energy of the optimized structure of $Si_2O_2(OH)_4$, will therefore probably be an underestimate. Care must be taken too when using the calculated potential for distortion of the SiOSiO unit from similar calculations on molecules such as **9** for the same reasons (vide Figure 11). A result very similar to that of Figure 11 is found for the silica-w chain.

The synthesis of the molecule **8**, and the determination of its structure, generated the suggestion[24] of a Si–Si bond across the SiOSiO unit. The distance is shorter than the value found for a normal Si–Si single bond. In our calculations we find no evidence from the sign of either Si–Si (or indeed O–O) bond overlap populations of any strong transannular attraction that would be called a bond. The molecule appears to be held together by conventional two-center–two-electron bonds, albeit in a strained environment.

Conclusions

The way we have tackled the energetics associated with these structures has shown quite dramatically that the geometric details are determined to quite a large extent by the energetics of the anionic lattice—a matrix effect. The observed geometry is close to that predicted by minimizing the energy of the anions alone. This occurs at either the maximum volume geometry or one close to it, subject to the constraint of constant anion–cation distance. However, we should realize that this assessment has largely come

---

(23) Canadell, E.; Eisenstein, O. *Inorg. Chem.* **1983**, *22*, 3856.

(24) Fink, M. J.; Haller, K. J.; West, R.; Michl, J. *J. Am. Chem. Soc.* **1984**, *106*, 822.

(25) (a) Hill, R. J.; Newton, M. D.; Gibbs, G. V. *J. Solid State Chem.* **1983**, *47*, 185. (b) Baur, W. H.; Khan, A. A. *Acta Crystallogr., Sect. B: Struct. Crystallogr. Cryst. Chem.* **1971**, *B27*, 2133.

(26) Weiss, V. A.; Weiss, A. *Z. Anorg. Allg. Chem.* **1984**, *276*, 95.

(27) Doubt has been cast on the existence of this structure.[3b] Indeed the reported structure has exceedingly long Si–O distances, longer than those found for six-coordinate silicon in stishovite. A structural redetermination of this material is clearly called for.

Table II

atom	orbital	H_{ii}, eV	exponent
Be	2s	−10.00	1.25
	2p	−6.00	1.25
C	2s	−21.4	1.625
	2p	−11.4	1.625
O	2s	−32.3	2.275
	2p	−14.8	2.275
Cl	3s	−30.0	2.033
	3p	−15.0	2.033
Si	3s	−17.3	1.383
	3p	−9.2	1.383
Pd	5s	−9.57	2.19
	5p	−3.43	2.15
	4d	−14.07	5.98 (0.5265), 2.613 (0.6372)[a]

[a] Double-ζ wave function; coefficients in parentheses.

about because of our elimination of "ligand–ligand" interactions in the calculation of the local energetic contribution at the cationic site. This is somewhat artificial since the geometries of free molecules are set by a combination of central-atom–ligand and ligand–ligand effects. In other words, the matrix effect, described in this paper, includes steric effects between the ligands that a molecular chemist would take for granted. On the other hand, there are many more close anion–anion contacts in the crystal, and their importance is correspondingly greater. An interesting result still is that the observed arrangement is one that concurrently satisfies local geometrical (often tetrahedral) and matrix requirements. We have described a similar situation for some molecular fragments in ref 1a. There we demonstrate an excellent correlation between the one-electron orbital energy associated with central-atom–ligand interaction and the energetics of ligand–ligand repulsions using the points-on-a-sphere model.[19b] The physical reasoning behind such a correspondence has yet to be elucidated.

Given the energetic importance of the matrix, the use of numerical data gleaned from calculations on molecular fragments needs to be interpreted carefully. The qualitative aspects of bond length/bond angle relationships, and indeed of the geometrical details of silicate structures elucidated so beautifully by Gibbs and co-workers[2,3,20] will clearly still hold, but the use of potential function data, derived from systems where only a fraction of the close contacts of the solid are included, may well not be a good way to quantitatively model either bulk properties or the energy difference between systems with very different crystal structures. A complicating factor here too is that the stoichiometry of the fragment chosen is, of necessity, not that of the crystal itself.

Acknowledgment. This research was supported by the National Science Foundation, Grant Nos. NSF DMR 8019741 and NSF DMR 8216892. D.C.C. was also supported by a generous grant from the Richter Fund.

Appendix

All of the calculations described in this paper used the extended Hückel method both for the molecular orbital calculations on the fragments torn from the crystal lattice and for the tight-binding computations on the crystalline materials. The parameters are given in Table II.

All the calculations involving geometrical deformations maintained constant nearest-neighbor anion–cation distances. These were as follows: Be–O, 1.60 Å; Pd–O, 1.95 Å; Si–O, 1.62 Å for quartz and tridymite, 1.70 Å for silica-w (this is close to the average distance in the molecule **8**[24]), and 1.77 Å for stishovite (this is the average of the symmetry-inequivalent distances in the crystal[25]); Pd–Cl, 2.309 Å. Sufficient *k* points were included to achieve energetic convergence. For the calculations on β-quartz, for example, a set of eight points within the irreducible wedge of the hexagonal Brillouin zone was found to be adequate. The lattice sums of the tight-binding calculations were invariably over two unit cells in all three directions. In two of the calculations on β-quartz, however, no interactions were included beyond 3 Å, in an attempt to gauge the importance of direct silicon–silicon interactions.

Registry No. BeO, 1304-56-9; $PdCl_2$, 7647-10-1; PtS, 12038-20-9; PtO, 12035-82-4; PdO, 1314-08-5; SiO_2, 7631-86-9; cooperite, 12197-03-4; β-tridymite, 15468-32-3; β-quartz, 14808-60-7; stishovite, 13778-37-5.

Contribution from the Departimento di Chimica Generale,
Università di Pavia, 27100 Pavia, Italy

Formation of a Trivalent Silver Tetraaza Macrocyclic Complex in Aqueous Solution: Hydrolytic Tendencies and Interaction with the Sulfate Ion

MARIA PESAVENTO, ANTONELLA PROFUMO, TERESA SOLDI, and LUIGI FABBRIZZI*

Received January 18, 1985

The Ag^{II} complex with the tetraaza macrocycle **1** in aqueous solution undergoes a reversible one-electron-oxidation process to give an authentic Ag^{III} species. The Ag^{III}/Ag^{II} redox couple potential (0.835 V vs. Ag/AgCl) is affected by variation of the acidity of the solution, indicating that the Ag^{III}(**1**) complex behaves as a fairly strong acid (pK = 2.6). The positive value of the reaction entropy for the $[Ag^{III}(\mathbf{1})]^{3+}/[Ag^{II}(\mathbf{1})]^{2+}$ redox couple, measured with a nonisothermal method, indicates that the water molecules must be present in the coordination sphere of the trivalent complex. Presence of sulfate in solution stabilizes the Ag^{III} complex due to the formation of a 1:1 adduct.

Introduction

The disproportionation reaction of Ag^+, eq 1, in the presence of a 14-membered tetraaza macrocycle such as **1** to give a silver mirror and a yellow solution of the Ag^{II} tetraaza macrocyclic complex, was independently discovered by Allred[1] and Barefield.[2]

$$2Ag^{I} + \mathbf{1} \rightleftharpoons [Ag^{II}(\mathbf{1})]^{2+} + Ag \qquad (1)$$

This distinctive aspect of the coordination chemistry of silver reflects the tendency of cyclic tetraaza ligands to establish strong in-plane metal–nitrogen interactions, according to a tetragonal stereochemistry: the transition-metal ion Ag^{II} (electronic configuration d^9) profits to such a large extent from this effect that the Ag^{I}/Ag^{II} oxidation process can be accomplished even by a smooth oxidizing agent such as Ag^{I}.

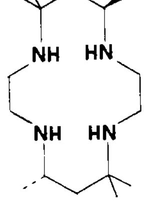

1

---

[1] Kestner, M. O.; Allred, A. L. *J. Am. Chem. Soc.* **1972**, *94*, 71.
[2] Barefield, E. K.; Mocella, M. T. *Inorg. Chem.* **1973**, *12*, 78.